

# RSC Advances



This is an *Accepted Manuscript*, which has been through the Royal Society of Chemistry peer review process and has been accepted for publication.

*Accepted Manuscripts* are published online shortly after acceptance, before technical editing, formatting and proof reading. Using this free service, authors can make their results available to the community, in citable form, before we publish the edited article. This *Accepted Manuscript* will be replaced by the edited, formatted and paginated article as soon as this is available.

You can find more information about *Accepted Manuscripts* in the [Information for Authors](#).

Please note that technical editing may introduce minor changes to the text and/or graphics, which may alter content. The journal's standard [Terms & Conditions](#) and the [Ethical guidelines](#) still apply. In no event shall the Royal Society of Chemistry be held responsible for any errors or omissions in this *Accepted Manuscript* or any consequences arising from the use of any information it contains.

1  
2  
3  
4  
5  
6  
7  
8  
9  
10  
11  
12  
13  
14  
15  
16  
17  
18  
19  
20  
21  
22  
23  
24  
25  
26

**Comparative study of preparation, characterization and anticandidal activities of chitosan silver nano composite (CAgNC) compared with low molecular weight chitosan (LMW-chitosan)**

Dananjaya S.H.S<sup>a</sup>, Kulatunga D.C.M<sup>a</sup>, G.I. Godahewa<sup>b</sup>, Jehee Lee<sup>b</sup>, Mahanama De Zoysa<sup>a,b\*</sup>

<sup>a</sup>College of Veterinary Medicine and Research Institute of Veterinary Medicine, Chungnam National University, Yuseong-gu, Daejeon, 305-764, Republic of Korea.

<sup>b</sup>Fish Vaccine Research Center, Jeju National University, Jeju Self-Governing Province 690-756, Republic of Korea.

\* Corresponding author:

Mahanama De Zoysa

College of Veterinary Medicine and Research Institute of Veterinary Medicine, Chungnam National University, Yuseong-gu, Daejeon, 305-764, Republic of Korea.

Tel:+82428216795; Fax:+82428218903

E-mail:mahanama@cnu.ac.kr; (De Zoysa, M)

RSC Advances Accepted Manuscript

27  
28  
29  
30  
31  
32  
33  
34  
35  
36  
37  
38  
39  
40  
41  
42  
43  
44  
45  
46  
47  
48  
49

### Abstract

Chitosan-silver nanocomposite (CAgNC) was green synthesized using low molecular weight chitosan (LMW-chitosan) and silver nitrate without applying external chemical-reducing agents. The newly synthesized CAgNC was characterized by UV-visible spectroscopy, fourier transform infrared spectroscopy (FT-IR), X-ray diffraction (XRD), field emission electron microscopy (FE-SEM and FE-TEM), inductively coupled plasma-atomic emission spectroscopy (ICP-AES), particle size and zeta potential analysis. The average size of LMW-chitosan and CAgNC were  $1776 \pm 23$  nm and  $240.1 \pm 23.6$  nm, respectively. The zeta potential of CAgNC was observed as + 41.1 mV. The AgNPs which are deposited on chitosan matrix had average size ranges between 5-50 nm. The Ag content of the CAgNC was determined as  $0.696 \pm 0.054\%$  (w/w). The minimum inhibitory concentration (MIC) values of LMW-chitosan and CAgNC against *Candida albicans* were determined as 100 and 50  $\mu\text{g/mL}$ , whereas the minimum fungicidal concentration (MFC) values were recorded as 400 and 150  $\mu\text{g/mL}$ , respectively. Propidium iodide (PI) uptake results suggested that CAgNC has affected to permeability of cell membrane of *C. albicans*. Moreover, CAgNC induced the level of reactive oxygen species (ROS) at higher level when compared to the LMW-chitosan in concentration dependent manner. This report illustrates the eco-friendly approach for the reduction of silver ions using LMW-chitosan as a reducing agent to make biologically active composite (CAgNC) and as potential antifungal agent against *C. albicans*.

**Keywords:** Low molecular weight chitosan (LMW-chitosan); chitosan silver nano composite (CAgNC); Silver nano particles (AgNPs); antifungal agent; *C. albicans*.

## 50 1. Introduction

51 Chitosan, a natural cationic polysaccharide which is consisted of co-polymers of glucosamine ( $\beta$   
52 1–4-linked 2-amino-2-deoxy-d-glucose) and N-acetyl glucosamine (2-acetamido-2-deoxy-d-  
53 glucose). Chitosan is derived from partial deacetylation of chitin obtained from crustaceans or  
54 the mycelium of fungi.<sup>1</sup> Bacteriostatic<sup>2</sup> and fungistatic effects<sup>3</sup> due to reactive amino groups and  
55 metal ion chelating activity associated with linear polyamine (poly- D-gulcosamine) structures  
56 are the main functional properties of chitosan. Recently, applications of chitosan have extended  
57 to various fields such as medicine, food, chemical engineering, pharmaceuticals, nutrition,  
58 environmental protection and agriculture.<sup>4</sup> In particular, the antifungal and antibacterial activities  
59 of chitosan have been investigated against wide range of pathogenic strains.<sup>5</sup> The size and zeta  
60 potential of chitosan particles are critical properties when considering its bioactivities.<sup>6</sup>

61 Nanosilver (silver nanoparticles, AgNPs, or Ag<sup>0</sup><sub>nano</sub>) is considered as zero valent silver  
62 (Ag<sup>0</sup>) having a less than 100 nm of particle diameter. AgNPs are commonly synthesized through  
63 chemical reduction methods in which silver salts, such as AgNO<sub>3</sub>,<sup>7</sup> or silver perchlorate/AgClO<sub>4</sub>,<sup>8</sup>  
64 can be reduced by reducing agent like glucose,<sup>7</sup> or sodium borohydride/NaBH<sub>4</sub>.<sup>9</sup> In function,  
65 AgNPs displays stronger, longer-term, and broader spectrum of antimicrobial activities when  
66 compare with other metallic nano particles.<sup>10</sup> Meanwhile coating agents or stabilizers, such as  
67 polysaccharides,<sup>11</sup> poly vinyl alcohol/PVA,<sup>12</sup> poly ethylene glycol/PEG,<sup>13,14</sup> or citrate,<sup>15</sup> are  
68 generally used to prevent aggregation of AgNPs. To achieve better biomedical performances  
69 AgNPs, many researches have tested polymer based composite materials combined with  
70 AgNPs.<sup>16</sup>

71 Moreover, polymer embedded AgNPs have been shown superior characteristics such as  
72 longer stability, better dispersion and low toxicity levels. Chitosan-silver nano composite

73 (CAgNC) is one of the composite materials which can be synthesized via electrochemical,<sup>17</sup>  
74 chemical,<sup>18</sup> green synthesis,<sup>19,20</sup> and biosynthesis methods.<sup>21</sup> It possesses antimicrobial activity,  
75 <sup>22,23</sup> bio sensing potential,<sup>22</sup> and dye oxidation properties<sup>24</sup>. In recent years, severe fungal  
76 infections have caused increasing morbidity and mortality among immunocompromised patients  
77 who need intensive treatments.<sup>25</sup> *C. albicans* is the most widespread species among other  
78 Candida species such as *C. tropicalis*, *C. glabrata*, *C. krusei*.<sup>26</sup> Therefore, it is an urgent need  
79 for development of new and non-toxic antifungal agents against, *C. albicans*.

80 Our main objective of the present study was to compare the physio-chemical properties  
81 and anticandidal properties of CAgNC with its precursor LMW-chitosan. For that we firstly  
82 prepared the CAgNC using LMW-chitosan and determined the physiochemical properties such  
83 as particle size, zeta potential, UV-vis absorption, FE-SEM, FE-TEM and XRD. In order to  
84 make functional comparison, antifungal activity against *C. albicans* was assessed under various  
85 parameters such as MIC, MFC, cell viability, change of cell membrane structure, capacity of  
86 ROS production and PI uptake. Based on the results and interpretation of possible mode of action,  
87 we conclude that newly synthesized CAgNC has superior antifungal activities than LMW-  
88 chitosan.

## 89 **2. Experimental section**

### 91 **2.1 Synthesis and characterization of CAgNC from LMW-chitosan**

92 CAgNC was green synthesized by reduction method using LMW(50-150 kDa)-chitosan  
93 with a deacetylation degree of ~85% (Sigma–Aldrich, USA). In brief, the CAgNC was  
94 synthesized by adding 4 mL of freshly prepared 0.01 M AgNO<sub>3</sub> solution (Sigma Aldrich, USA)  
95 followed by addition of 400 µL of 0.5 M NaOH solution (Biosesang, Korea) to 100 ml of 0.2%  
96 (w/v) LMW-chitosan solution with constant stirring at 95 °C. The formation of AgNPs was

97 indicated by the appearance of a yellow color about 1 min after the addition of the NaOH  
98 solution. After 15 min, the resulting suspension was filtered and washed several times using  
99 distilled water and then dried at 60 °C for 6 h. In order to confirm the formation of AgNPs,  
100 UV–Vis spectroscopy was carried out using double beam UV–vis spectrophotometer (Mecasys,  
101 Korea), over a range of 300- 800 nm. The percentage of Ag in CAgNC was determined using an  
102 ICP–AES (Perkin-Elmer Optima, USA). FT-IR spectra was recorded in the wavelength region  
103 4000-600 cm<sup>-1</sup> using Bio-Rad 175 C FTS spectrophotometer in Attenuated Total Reflectance  
104 (ATR) mode. The surface morphology was examined by FE-SEM analysis (Hitachi S-4800,  
105 Japan) operating at an accelerating voltage of 3.0 kV. The particle size and shape of the CAgNC  
106 was analyzed using FE-TEM, (Model Tecnai G2 F30 S-Twin, FEI, USA) operating at 300 keV.  
107 The phase analysis was done by observing the SAED pattern to confirm the crystal structure of  
108 CAgNC. X-ray diffraction (XRD) is a versatile, non-destructive analytical method for the  
109 identification and quantitative determination of various crystalline phases. Powder XRD analysis  
110 was conducted via Philips PW 1710 diffractometer with Cu K $\alpha$  radiation ( $\lambda = 1.5406 \text{ \AA}$ ) and  
111 graphite monochromator, operated at 45 kV; 30 mA and 25 °C. Particle size distribution and zeta  
112 potential of CAgNC and LMW-chitosan were determined by Zetasizer S-90 Malvern instruments  
113 (Malvern, UK) using diluted and dispersed solution of CAgNC in 0.25 % (V/V) acetic acid.

114

## 115 **2.2 Analysis of anticandidal activities of CAgNC and LMW-chitosan**

116 MIC and MFC of CAgNC and LMW -chitosan against *C. albicans* were determined via  
117 turbid metric assay as described previously.<sup>28</sup> The different concentrations of CAgNC and  
118 LMW-chitosan (25, 50, 75, 100, 150 and 200  $\mu\text{g/mL}$ ) were added to 4 mL of potato dextrose  
119 broth (PDB, Difco-USA) with *C. albicans* at 0.05 OD: 600 nm ( $10^5$  CFU/mL) and incubated at

120 30 °C while shaking at 150 rpm for 24 h. The corresponding control test was carried out without  
121 CAgNC and LMW-chitosan, whereas the positive control was conducted with 10 µg/mL  
122 Nystatin. All experiments were carried out in triplicates.

123

### 124 **2.3 Determination of ROS production and cell viability**

125 To determine the ROS production and the cell viability in *C. albicans* culture (0.05 OD,  
126 600nm) with different concentrations of CAgNC and LMW-chitosan (0 to 100 µg/mL) was kept  
127 in a shaking incubator for 6 h at 30 °C. ROS generated cells were stained with 30 µg/mL 5-(and-  
128 6)-carboxy-2',7' dichloro dihydro fluorescein diacetate (H<sub>2</sub>DCFDA) followed by 30 min  
129 incubation and harvesting by centrifugation at 13000 rpm for 2 min. Cells were washed and  
130 dissolved using ×1 PBS to quantify ROS generation using the FACScaliber flow cytometer  
131 (Becton Dickinson, USA). Cell viability was determined by MTT assay. Briefly, after 24 h  
132 incubation period, the samples were treated with 70 µg/µL of MTT solution (3-(4, 5-dimethyl-2-  
133 thiazolyl)-2, 5-diphenyl-2H-tetrazolium bromide) and incubated for additional 30 min. Harvested  
134 cells were re-suspended in DMSO (200 µg/µL well<sup>-1</sup>) and cell viability was detected at OD 570  
135 using a micro plate reader (Thermo, USA) attached to a computer.

136

### 137 **2.4 Effect on CAgNC and LMW-chitosan on plasma membrane of *C. albicans* by PI assay**

138 Cell membrane integrity of CAgNC and LMW-chitosan treated *C. albicans* was assessed  
139 by monitoring the uptake of the fluorescent probe, PI (Sigma Aldrich, USA). For the  
140 determination of the PI uptake, cell suspensions of the control, MIC and MFC levels treated  
141 samples were centrifuged (3500 rpm, 2 min,) and the pellets were re-suspended in PBS. The  
142 treated cells were incubated with PI (5 µg/mL) at 30 °C for 15 min in dark. Over staining were

143 washed twice with PBS. Finally, one drop of each suspensions was placed on the cover slip and  
144 observed using a Zess LSM 510 meta confocal laser scanning microscope (CLSM) scan head  
145 integrated with the Axiovert 200 M inverted microscope (Carl Zeiss, Jena, Germany). *C.*  
146 *albicans* cells were observed through a 40 x 1.3 oil objective and PI was excited with the 543  
147 laser line and the emission was recorded through a 585 long-pass filter.

148

## 149 **2.5 Statistical analysis**

150 All the data related to the cell viability was illustrated as means  $\pm$  SD for triplicate  
151 reactions. Statistical analysis was performed using unpaired, two-tailed *t*-test to calculate the *P*-  
152 value using GraphPad program (GraphPad Software, Inc.). The significant difference was  
153 defined at  $P < 0.05$ .

## 154 **3. Result and discussion**

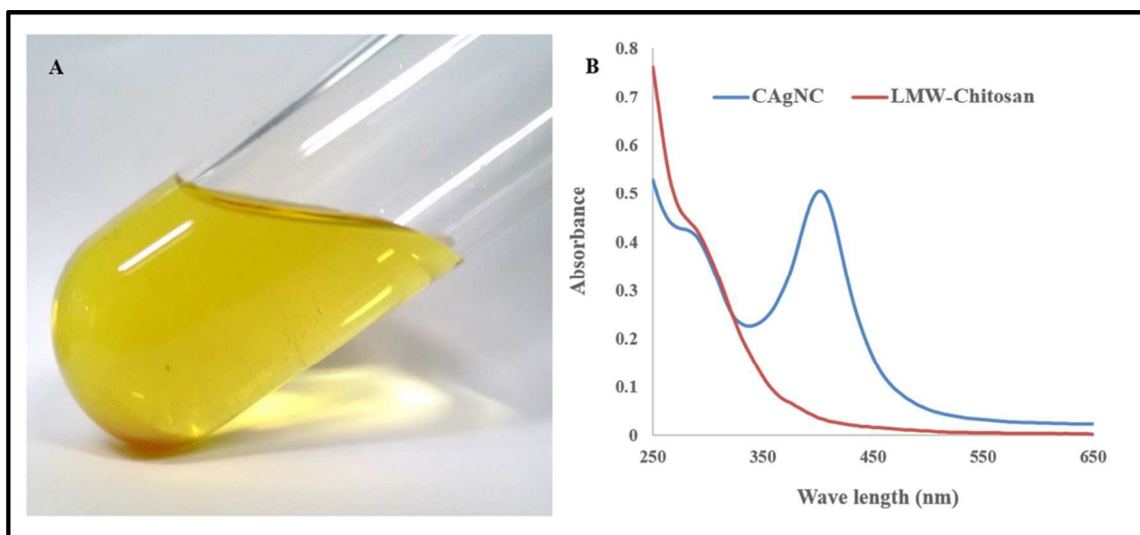
### 155 **3.1 Synthesis and characterization of CAgNC**

156 Present study describes the use of LMW-chitosan with AgNPs to develop biologically active and  
157 superior anticandidal agent against *C. albicans*. The first part of this work is synthesis of CAgNC  
158 using LMW-chitosan and physiochemical characterization. The progress of the AgNPs synthesis  
159 was tracked by using UV–Vis spectroscopy. The UV–visible absorption spectra of LMW-  
160 chitosan and CAgNC are shown in Fig. 1. The spectra exhibited an absorption band around 415  
161 nm for CAgNC. However, there is no specific absorption spectrum observed in LMW-chitosan.  
162 The surface plasmon resonance (SPR) band of spherical AgNPs was observed around 420 nm  
163 and it clearly evidences for the formation of AgNPs as previously reported.<sup>29</sup> To convert the  $\text{Ag}^+$   
164 into metallic Ag, an electron supplier or a reducing agent should be added. When NaOH is added



165 to an  $\text{AgNO}_3$  aqueous solution, the pH of the solution can be increased and  $\text{Ag}_2\text{O}$  is precipitated  
166 as solid mass.<sup>30</sup> However, in this study, a solid gray precipitate of  $\text{Ag}_2\text{O}$  was not formed because  
167  $\text{Ag}^+$  stabilized by the basic chitosan suspension. Then  $\text{Ag}^+$ /chitosan complex has allowed  $\text{Ag}^+$   
168 to collect electrons from the basic suspension and to be reduced to an Ag atom. Twu et al<sup>20</sup>, has  
169 suggested the greater probability of supplying electron by degradation products of low-molecular  
170 weight chitosan (e.g. glucosamide) and functioning as a reducing agent.

171



172

173 **Fig 1.** Product of CAgNC and UV-visible spectroscopy analysis. (A) Formation of AgNPs on  
174 chitosan matrix which develops yellow color. (B) UV-Vis spectrum of AgNPs presenting an  
175 absorption peak at 410 nm due to surface plasma resonance (LMW-Chitosan as pre-causer).

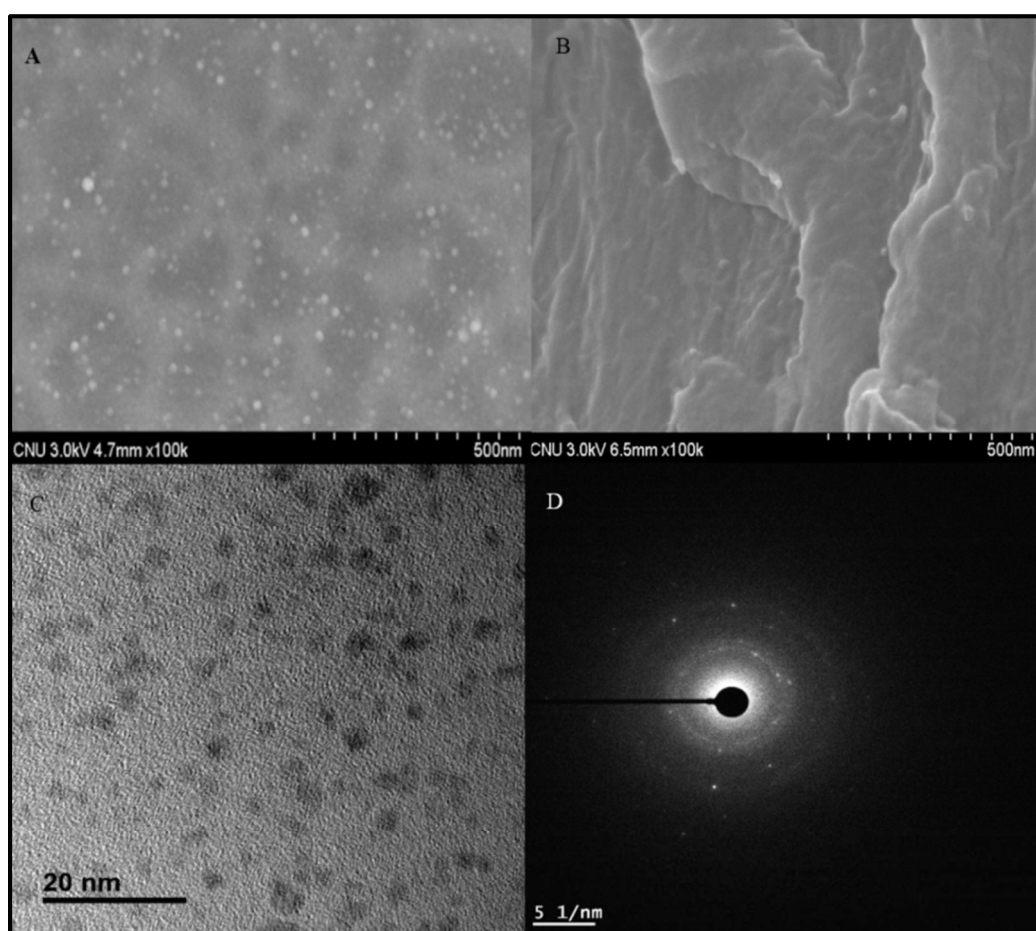
176 We studied the chemical interaction between LMW-chitosan and Ag in the CAgNC matrix by  
177 FT-IR spectral analysis. Results show the FT-IR spectrum of CAgNC indicating the band at  
178  $3366\text{ cm}^{-1}$  which confirms the stretching vibrations of -OH and -NH groups (Fig. S1). Moreover,  
179 additional bands were displayed at  $2871\text{ cm}^{-1}$ ,  $1645\text{ cm}^{-1}$ ,  $1375\text{ cm}^{-1}$ ,  $1060\text{ cm}^{-1}$  which are  
180 ascribed to the asymmetric stretching vibrations of -CH group, amide group (C-O stretching

181 along-N-H deformation), COO<sup>-</sup> group carboxylic acid salt, and stretching vibrations of C-O-C  
182 in the glucose unit, respectively. The LMW-chitosan shows all the corresponding bands of  
183 CAgNC. However, the spectrum of the CAgNC was shifted towards lower wave numbers (amine  
184 group was shifted from 1658 cm<sup>-1</sup> to 1645 cm<sup>-1</sup>) when compare with the spectrum of LMW-  
185 chitosan. This suggests the attachment of Ag into N atoms (amino groups), which reduces the  
186 vibration intensity of the N-H bond due to the greater molecular weight of CAgNC due to the  
187 incorporation of Ag atoms in to LMW-chitosan as described previously.<sup>31</sup>

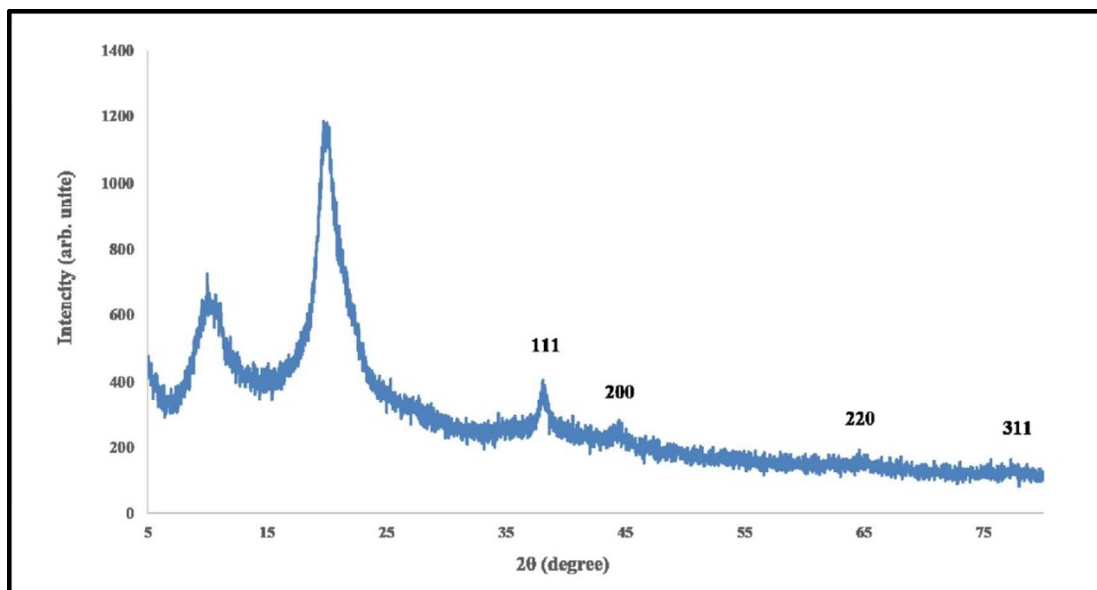
188 The surface morphology of the synthesized CAgNC and LMW-chitosan was analyzed  
189 using FE-SEM and images are presented in Fig. 2 A & B. The FE-TEM image (Fig. 2 C)  
190 implies the presence of spherical AgNPs in the chitosan suspension. Also, it clearly indicated  
191 that AgNPs were deposited on chitosan matrix and the average particle size of AgNPs lies  
192 between 5-50 nm. The three *diffraction* patterns observed in the selected area of electron  
193 diffraction (SAED) pattern are shown in Fig. 2 D, and it can be indexed to a face centered cubic  
194 lattice. The first strongest ring is the combination of both (111) and (200) planes, whereas the  
195 second ring corresponds to the crystallographic plane of (220). The third ring represents the  
196 (311) plane of Ag. The SAED pattern was completely aligned with the XRD pattern.

197 XRD is a versatile and non-destructive analytical method for the identification and  
198 quantitative determination of various crystalline phases. The structural properties of CAgNC  
199 were analyzed using XRD technique. XRD analysis results revealed that pattern of CAgNC was  
200 clearly differed from that of LMW-chitosan (Fig. 3). The peak for LMW-chitosan was appeared  
201 at 2 $\theta$  value of the broad peak around 5°–25° (Fig. S2). The XRD pattern of powdered CAgNC  
202 showed Bragg reflections with 2 $\theta$  values of 38.12, 44.22, 64.36 and 77.32 for a set of lattice  
203 planes which could be indexed to (1 1 1), (2 0 0), (2 2 0) and (3 1 1) planes of face centered cubic

204 geometry of Ag and the existence of broad peak between  $5^{\circ}$ – $25^{\circ}$  which can be attributed to the  
205 presence of LMW-chitosan in the CAgNC. The results showed that the synthesized CAgNC  
206 contains AgNPs in crystalline structure, since the position and the relative intensity of all the  
207 diffraction peaks of the samples were consistent with the crystalline pattern of Ag.<sup>32</sup> The lattice  
208 parameters were determined to be  $a = 4.0580$  that matches with the Joint Committee on Powder  
209 Diffraction Standards (JCPDS) file no. 87– 0720. There were no additional peaks in the spectra,  
210 indicating the purity of CAgNC sample and no detectable impurities present.



211  
212 **Fig. 2.** The FE-SEM and FE-TEM image of CAgNC. (A) FE-SEM image of CAgNC (B) FE-  
213 SEM image of LMW-chitosan (C) FE- TEM image of CAgNC (D) SEAD pattern of CAgNC.



214

215 **Fig. 3.** The XRD graph of the CAgNC.

216 The particle size distribution of LMW-chitosan and CAgNC was determined using  
 217 Zetasizer Nano-ZS90. The analysis was performed in triplicates for each sample and presented as  
 218 mean  $\pm$  standard deviation (SD) in table 1. Agreeing to the result of this analysis, the average  
 219 size of LMW-chitosan and CAgNC were  $1776 \pm 23$  nm and  $240.1 \pm 23.6$  nm, respectively (Fig.  
 220 S3A & S3B). Zeta potential of synthesized CAgNC measured at pH = 4.6 was found as + 41.1  
 221 mV (Fig. S3C). The value of zeta potential enables determination of colloid stability and particle  
 222 aggregation.<sup>33</sup> Therefore, the positive value of the zeta potential of CAgNC could have  
 223 evidenced the presence of positively charged polymeric layer on AgNPs surface.

224

### 225 3.2 Anticandidal of LMW-chitosan and CAgNC

226 After characterization of CAgNC, we investigated the antifungal activity against *C.*  
 227 *albicans*. The synthesized CAgNC showed superior antifungal activity against *C. albicans*  
 228 compared to LMW-chitosan. It was found that MIC and MFC of LMW-chitosan as 100 400  
 229  $\mu\text{g/mL}$ , respectively (Table 1).

230

231 **Table 1.** Comparison of particle size, zeta potential, MIC and MFC of LMW-chitosan and  
 232 CAgNC.

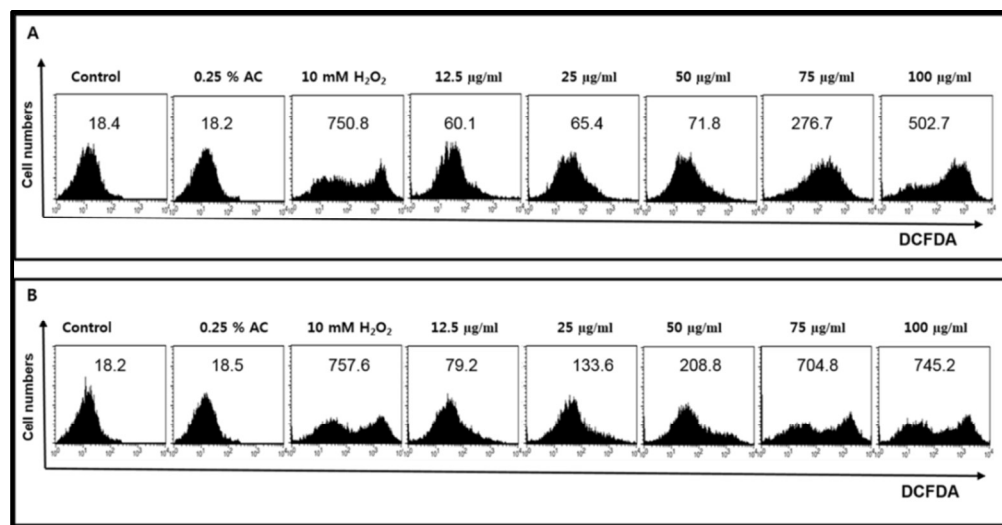
Compound name	Particle size (nm) (Mean $\pm$ SD)	Zeta potential (mV) (Mean $\pm$ SD)	MIC ( $\mu\text{g/mL}$ )	MFC ( $\mu\text{g/mL}$ )
LMW-chitosan	1776 $\pm$ 23.00	-----	100	400
CAgNC	240.1 $\pm$ 23.26	+ 41.6 $\pm$ 4.64	50	150

233

234 Interestingly CAgNC showed significantly lower MIC of 50  $\mu\text{g/mL}$  (2 times lower than  
 235 LMW-chitosan) and MFC of 150  $\mu\text{g/mL}$  (2.7 times lower than LMW-chitosan), respectively. Ing  
 236 et al.,<sup>34</sup> showed that LMW-chitosan solution has higher MIC<sub>90</sub> value (3 mg/ml) compare with  
 237 chitosan nano particle (0.25 mg/ml) against *C. albicans*. Panacek et al.,<sup>25</sup> showed that MIC of  
 238 stabilized AgNPs varied from 0.052 to 0.84 mg/L with *Candida sp.* The size of particles plays an  
 239 important role in determination of antimicrobial activity of nanoparticles as they enter the cell  
 240 walls of microbes through carrier proteins or ion channel and smaller nanoparticles result in a  
 241 better uptake into microbial cells<sup>6</sup>. Zeta potential has been suggested as a key factor that is  
 242 contributing to antifungal effect of chitosan through the interaction with negatively charged  
 243 microbial surface.<sup>35</sup> The synthesized CAgNC has shown higher anticandidal activity because of  
 244 its low particle size and higher zeta potential value when compare with LMW-chitosan. The  
 245 mode of action of CAgNC against *C. albicans* is not fully understood and therefor further  
 246 investigations are required to establish in future.

247 Recent study<sup>36</sup> suggested that the accumulation of ROS induces and regulates the  
 248 apoptotic pathway in yeast. Thus, to examine the relationship between the accumulation of ROS  
 249 and the induction of apoptosis, an experiment was conducted to find out the effect of different  
 250 concentration of LMW-chitosan and CAgNC on the ROS production and cell viability in *C.*

251 *albicans*. ROS level was slightly increased until 75  $\mu\text{g/mL}$  and beyond 100  $\mu\text{g/mL}$  (for LMW,  
 252 MIC is 100  $\mu\text{g/mL}$ ) in LMW-chitosan treated (12.5, 25, 50 and 75  $\mu\text{g/mL}$ ) *C. albicans*. (Fig. 4).  
 253 Furthermore, *C. albicans* samples which were treated with 12.5  $\mu\text{g/mL}$  and 25  $\mu\text{g/mL}$   
 254 concentrations of CAgNC have demonstrated sequentially increased ROS levels. Also, at 50  
 255  $\mu\text{g/mL}$  (MIC of 50  $\mu\text{g/mL}$  for CAgNC) a steep increase was observed while it slightly increased  
 256 again at 100  $\mu\text{g/mL}$ . Moreover similar ROS values were obtained both control and acetic acid  
 257 treated samples as well as for positive control (10 mM  $\text{H}_2\text{O}_2$ ) treated samples. Further, ROS  
 258 result showed slight increased value for CAgNC treated sample comparing to the LMW-  
 259 chitosan. The reason for such observation could be that AgNPs have the capacity to inhibit the *C.*  
 260 *albicans* by increasing the oxidative stress.



261  
 262 **Fig. 4.** Effect of LMW-chitosan and CAgNC on ROS production in *C. albicans* cells. A) LMW-  
 263 chitosan B) CAgNC. 0.25 % (V/V). AC: acetic acid (Negative control), 10 mM  $\text{H}_2\text{O}_2$  (Positive  
 264 control).

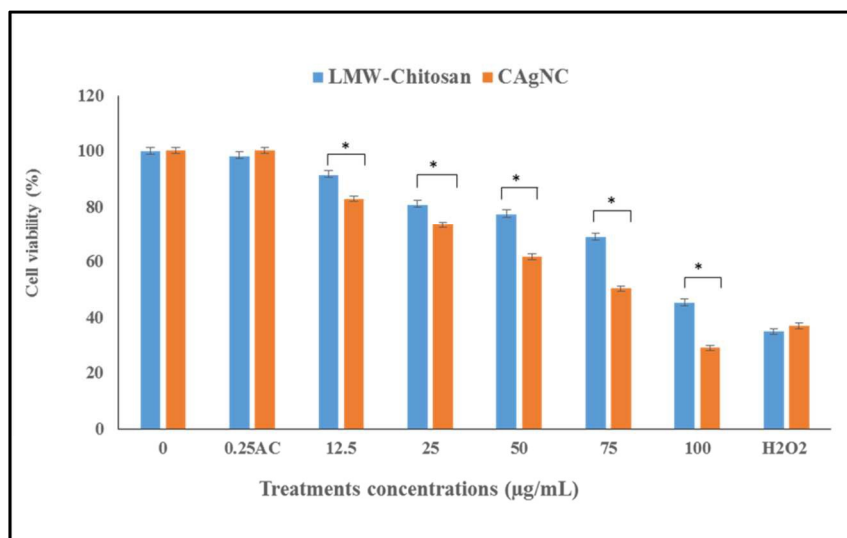
265 The overall results suggest that LMW-chitosan and CAgNC trigger the oxidative stress  
 266 by generating ROS which causes various damages to macromolecules such as DNA, RNA, and  
 267 proteins as well as other cellular components.<sup>36,37</sup> The production of ROS may be interfered with

268 the essentials of electronic transport chain which may cause the reduction of cellular energy  
269 production.<sup>38</sup> Additionally, the excessive production of ROS may damage plasma membrane and  
270 intra cellular organelles which may leads to cell death.<sup>39</sup> The cell viability of *C. albicans* was  
271 decreased significantly ( $P < 0.001$ ) with increasing the concentration of LMW-chitosan and  
272 CAgNC (Fig. 5). Furthermore, highest and lowest cell viability in LMW-chitosan treatment was  
273 observed in control and  $H_2O_2$  treated groups, respectively. Whereas highest and lowest cell  
274 viability was observed in control and 100  $\mu\text{g/mL}$  of CAgNC treated group, respectively. All the  
275 CAgNC treated groups were shown lower cell viability than LMW-chitosan. However,  
276 significant difference ( $P < 0.05$ ) in cell viability was observed in CAgNC and LMW-chitosan  
277 treatments from 12.5 ~100  $\mu\text{g/mL}$  concentration. Thereby, lowest cell viability (28%) was  
278 observed in 100  $\mu\text{g/mL}$  CAgNC treatment. Whereas, cell viability for positive control was 34 %  
279 at the 10 mM  $H_2O_2$  and negative control 100 % at 0.25 % AC.

280 The PI uptake result is associated with the occurrence of substantial damage to the  
281 membrane, indicating alteration of cell membrane potential, which finally causes cell death. PI  
282 could enter the cell and bind to DNA, showing red fluorescence.<sup>40</sup> PI uptake by *C. albicans* cells  
283 show concentration dependent mortality in both treated groups where control and MIC treatment  
284 have the least number of PI stained *C. albicans* cells which indicates the least number of cell  
285 death (Fig. 4 S). However, almost all *C. albicans* cells in both treatments at the MFC level have  
286 shown higher red florescence (Fig. 6).

287





288

289 **Fig. 5.** Comparison of the effect of LMW-chitosan and CAgNC on cell viability of *C. albicans*.

290 Cell viability was assessed by MTT assay (n=3) after treatment with different concentration of

291 LMW-chitosan and CAgNC (12.5 –100 µg/mL). Significant differences in *C. albicans* cell

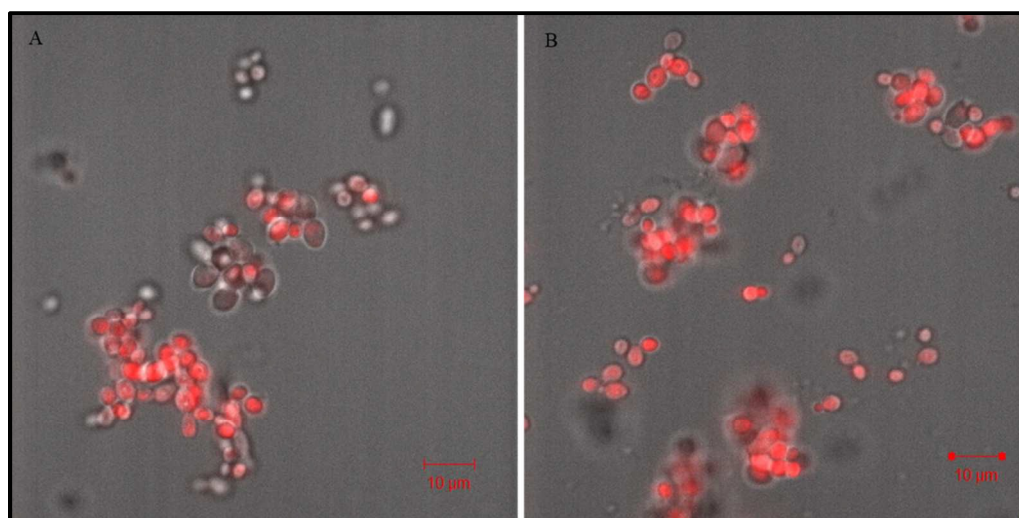
292 viability were obtained with respect to untreated control ( $P \leq 0.05$ ). The treatments with \* mark

293 represent the significant cell viability (%) between LMW-chitosan and CAgNC. Bars with no

294 asterisk were not significantly difference in cell viability. Acetic acid 0.25 % (V/V) as negative

295 control and, 10 mM H<sub>2</sub>O<sub>2</sub> as positive control.

296



297



298 **Fig. 6.** Effect of LMW-chitosan and CAgNCon cell membrane permeability by PI staining.  
299 Merged image of *C. albicans* (by confocal laser scanning microscopy) showing the dead *C.*  
300 *albicans* cells at MFC treatment level. (A) LMW-chitosan (400  $\mu\text{g}/\text{mL}$ ) (B) CAgNC (150  
301  $\mu\text{g}/\text{mL}$ ). When cationic chitosan bind to the negatively charge cell surface it may cause to  
302 increase hyperpolarization of the plasma membrane.<sup>41</sup> Also, some amount of AgNPs on the  
303 surfaces could be ionized and produce cationic silver ( $\text{Ag}^+$ ) traces. This  $\text{Ag}^+$  traces flowing in to  
304 the cell with the cationic influx generated due to hyperpolarized cell membrane.<sup>42</sup>

305

#### 306 **4. Conclusions**

307 In summary, we synthesized the CAgNC using LMW- chitosan without external chemical  
308 reducing agent and compared their physio-chemical properties and anticandidal action. First we  
309 prepared the improved version of chitosan nano composite format with unique characteristics  
310 such as smaller partical size (240.1 nm) higher zeta potential (+41.1 mV) and lower amount of  
311 AgNPs (0.69%). Moreover, CAgNC had superior anticandidal activities (MIC 50  $\mu\text{g}/\text{mL}$ , MFC  
312 100  $\mu\text{g}/\text{mL}$ ), than the preause LMW-chitosan suggesting that it has great potential to be  
313 developed as antifungal agent against wide array of Candida species.

314

#### 315 **Acknowledgements**

316 This work was supported by a National Research Foundation of Korea (NRF) grant funded by  
317 the Korea government (MSIP) (2014R1A2A1A11054585), research fund of Chungnam National  
318 University and part of the project titled ‘Development of Fish Vaccines and Human Resource  
319 Training’, funded by the Ministry of Oceans and Fisheries, Republic of Korea.

320

321 **References**

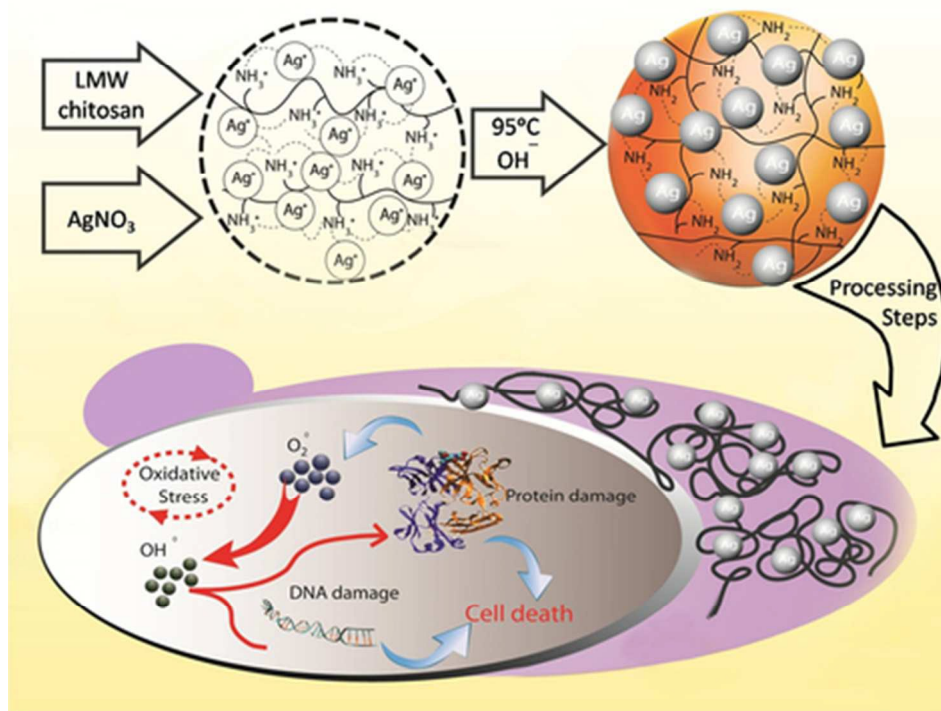
- 322 1. Y. Xia, Q.Fan, D. Hao, J.Wu, G. Ma, and Z. Su, *Vaccine.*, 2015. **33**, 5997–6010.
- 323 2. A. Nithya and K. Jothivenkatachalam, *J. Mater. Sci. Mater. Electron.*, 2015, **26**, 10207-
- 324 10216.
- 325 3. A.M.Soliman, S.R. Fahmy and W Mohamed, *J. Basic Appl. Zool.* 2015, in press.
- 326 4. S.C. Park, J.P. Nam, J.H. Kim, Y.M.Kim, J.W Nah and M.K.Jang, *Int. J. Mol. Sci.*, 2015,
- 327 **16**, 7995–8007.
- 328 5. R. C. Goy, S.T.B. Morais and B.G.A. Odilio, *Rev. Bras. Farmacogn.* 2015, in press.
- 329 6. D. Sharma, J. Rajput, B.S. Kaith, M. Kaur and S. Sharma, *Thin Solid Films*, 2010, **519**,
- 330 1224–1229.
- 331 7. X. Wang, Z.Ji, C.H.Chang, H. Zhang, M. Wang, Y.P. Liao, S. Lin, H. Meng, R. Li and B.
- 332 Sun, *Small.*, 2014,**10 (2)**, 385-398.
- 333 8. Y.Lee and S.G. Oh, *Colloids Surf. A Physicochem. Eng. Aspects.*, 2014, **459**, 172-176.
- 334 9. P.L. Freire, T.C. Stamford, A.J. Albuquerque, F.C. Sampaio, H.M. Cavalcante, R.O.
- 335 Macedo, A. Galembeck, M.A. Flores and A. Rosenblatt, *Int. J. Antimicrob. Agents.*, 2015,
- 336 **45 (2)**, 183-187.
- 337 10. M. Kooti, S. Gharineh, M. Mehrkhah, A.Shaker and H.Motamedi, *Chem. Eng. J.*, 2015. **259**,
- 338 34-42.
- 339 11. J.E. Skebo, C.M, Grabinski, A.M. Schrand, J.J. Schlager and S.M. Hussain, *Int. J. Toxicol.*,
- 340 2007, **26 (2)**, 135-141.
- 341 12. P.Khanna, N. Singh, D. Kulkarni, S.Deshmukh, S. Charan and P.Adhyapak, *Mater.Lett.*,
- 342 2007., **61 (16)**, 3366-3370.
- 343 13. L. Rizzello and P.P. Pompa, *Chem. Soc. Rev.*, 2014, **43(5)**, 1501-1518.

- 344 14. P. Simakova , J. Gautier, M. Proch-azka, K. Herve-Aubert and I. Chourpa, *J. Phys. Chem.*  
345 *C.*, 2014, **118 (14)**, 7690-7697.
- 346 15. M.N.Croteau, A.D. Dybowska, S.N.Luoma, S.K.Misra and E.Valsami-Jones, *Environ. Chem.*,  
347 2014, 11 (3), 247-256.
- 348 16. P. Dubey, B. Bhushan, A. Sachdev, I. Matai, S.U. Kumar and P.Gopinath, *J.Appl.polym.Sci.*,  
349 2015, **132**, 42473.
- 350 17. F.M.Reicha, A. Sarhan, M.I.Abdel-Hamid, I.M. El-Sherbiny, *Carbohydr. Polym.*, 2012, **89**,  
351 236–244.
- 352 18. H. Huang, Q. Yuan, X.Yang, *Colloids Surfaces B Biointerfaces.*, 2004, **39**, 31–37.
- 353 19. D.K.Boanic, L. V. Trandafilovic, A.S. Luyt, V.Djokovic, 2010. *React. Funct. Polym.*,  
354 2010, **70**, 869–873.
- 355 20. Y.K.Twu, Y.W. Chen and C.M. Shih, *Powder Technol.*, 2008, **185**, 251–257.
- 356 21. A.M.Youssef, M.S. Abdel-Aziz and S.M.El-Sayed, *Int. J. Biol. Macromol.*, 2014, **69**, 185–  
357 91.
- 358 22. S. Govindan, E. A. K. Nivethaa, R. Saravanan, V. Narayanan and A. Stephen, *Appl.*  
359 *Nanosci.*, 2012, 2, 299–303.
- 360 23. H.V.Tran, L.D.Tran, C.T. Ba, H.D.Vu, T.N. Nguyen, D.G. Pham and P.X. Nguyen,  
361 *Colloids Surfaces A Physicochem. Eng. Asp.*, 2010, **360**, 32–40.
- 362 24. J.Santhanalakshmi and V.Dhanalakshmi, *Indian. J. Sci.Tec.*, 2012, **15**, 3834–3838.
- 363 25. A.Panacek, M. Kolar, R. Vecerova, R. Pucek, J. Soukupova, V.Krystof, P. Hamal, R.  
364 Zboril and L. Kvitek, *Biomaterials.*, 2009, **30**, 6333–6340.
- 365 26. S.N.Kulikov, S.A. Lisovskaya, P. V. Zelenikhin, E. A.Bezrodnykh, D.R Shakirova, I.  
366 V.Blagodatskikh and V.E.Tikhonov, *Eur. J. Med. Chem.*, 2014, **74**, 169–178.

- 367 27. S.H.S. Dananjaya , G.I. Godahewa , R.G.P.T. Jayasooriya, J.Lee and M. De Zoysa,  
368 Aquaculture., 2016, **450**, 422–430.
- 369 28. E. G. Totoli and H. R. N. Salgado, *Pharmaceutics.*, 2015, 7, 106-121.
- 370 29. L. S.Wang, C.Y.Wang, C.H.Yang, C.L. Hsieh, S.Y.Chen, C.Y.Shen, J.J. Wang and K.S.  
371 Huang. *Int. J. Nanomedicine.*, 2015, **10**, 2685–2696.
- 372 30. D.K. Bonzanic, L.V. Trandfilovic , A.S Luyt and V. Djokovic, *Reac. Funct. Polymer.*,  
373 2010,**70**,869-873.
- 374 31. D.Wei, W.Sun, W.Qian, Y. Ye and X. Ma, *Carbohydr. Res.*, 2009, **344 (17)**, 2375–2382.
- 375 32. S.S. Sana, V.R. Badinni ,S.K Arala and V.K.N.Boya, *Materials Letters.*, 2015,**145**,347–350.
- 376 33. I. Ostolska and M. Wiśniewska, *Colloid Polym. Sci.*, 2014,**292**, 2453–2464.
- 377 34. L.Y, Ing, N.M. Zin, A. Sarwar. and H. Katas. *Int. J. Biomater.*, 2012. ID/632698.
- 378 35. L. C. Chen, S. K. Kung, H.H. Chen and S. B. Lin, *Carbohydr. Polym.*, 2010, **82**,913–919.
- 379 36. B. Hwang, J.S. Hwang, J. Lee, J.K. Kim, S.R., Kim, Y., Kim and D.G, Lee. *Biochem.*  
380 *Biophys. Res. Commun.*, 2011, **408**, 89–93.
- 381 37. C. Zhang, Z. Hu and B.Deng, *Water Res.*, 2016, **88**, 403–427.
- 382 38. E.D.Cavassin, L.F.P. de Figueiredo, J.P. Otoch, M.M.Seckler, R.A. de Oliveira, ,  
383 F.F.Franco, V.S. Marangoni, , V.Zucolotto, A.S.S. Levin and S.F.Costa, *J.*  
384 *Nanobiotechnology.*, 2015, **13**, 64.
- 385 39. G.G.Perrone, S.X.Tan and I.W. Dawes, *Biochim. Biophys. Acta - Mol. Cell Res.*, 2008,  
386 **1783**, 1354–1368.
- 387 40. A. Banerjee, P.Majumder, S.Sanyal, J.Singh, K.Jana, C.Das and D.Dasgupta, *FEBS Open*  
388 *Bio.*, 2014, **4**, 251–9.
- 389 41. A. Pena, N.S. Sanchez, M.Calahorra, *Biomed Res. Int.*, 2013, 527-549.

- 390 42. A. Ivask, A.Elbadawy,C.Kaweeteerawat,D.Boren, H. Fischer, Z.Ji,C.H.Chang, R.Liu,  
391 T.Tolaymat, D.Telesca, J. I.Zink,Y.Cohen, P.A.Holden, and H. A. Godwin, *ACS Nano.*,  
392 2014, **8**, 374–386.

393



39x32mm (300 x 300 DPI)